

SINTERED S53P4 BIOACTIVE GLASS SCAFFOLDS HAVE ANTI-INFLAMMATORY PROPERTIES AND STIMULATE OSTEOGENESIS *IN VITRO*

R. Björkenheim^{1,*}, E. Jämsen², E. Eriksson¹, P. Uppstu³, L. Aalto-Setälä⁴, L. Hupa⁴, K.K. Eklund^{2,5}, M. Ainola², N.C. Lindfors¹ and J. Pajarinen^{1,6}

¹Department of Musculoskeletal and Plastic Surgery, University of Helsinki and Helsinki University Hospital, Helsinki, Finland

²Translational Immunology Research Program, Faculty of Medicine, University of Helsinki, Helsinki, Finland

³Polymer Technology Research Group, Faculty of Science and Engineering, Åbo Akademi University, Turku, Finland

⁴Johan Gadolin Process Chemistry Centre, Åbo Akademi University, Turku, Finland

⁵Department of Rheumatology, Helsinki University and Helsinki University Hospital, and Orton Orthopedic Hospital and Research Institute, Helsinki, Finland

⁶Päijät-Häme central hospital, Department of Surgery, Lahti, Finland

Abstract

Bioactive glasses (BAG) are used as bone-graft substitutes in orthopaedic surgery. A specific BAG scaffold was developed by sintering BAG-S53P4 granules. It is hypothesised that this scaffold can be used as a bone substitute to fill bone defects and induce a bioactive membrane (IM) around the defect site. Beyond providing the scaffold increased mechanical strength, that the initial inflammatory reaction and subsequent IM formation can be enhanced by coating the scaffolds with poly(DL-lactide-co-glycolide) (PLGA) is also hypothesised. To study the immunomodulatory effects, BAG-S53P4 (\pm PLGA) scaffolds were placed on monolayers of primary human macrophage cultures and the production of various pro- and anti-inflammatory cytokines was assessed using reverse transcriptase quantitative polymerase chain reaction (RT-qPCR) and ELISA. To study the osteogenic effects, BAG-S53P4 (\pm PLGA) scaffolds were cultured with rabbit mesenchymal stem cells and osteogenic differentiation was evaluated by RT-qPCR and matrix mineralisation assays. The scaffold ion release was quantified and the BAG surface reactivity visualised. Furthermore, the pH of culture media was measured. BAG-S53P4 scaffolds had both anti-inflammatory and osteogenic properties that were likely attributable to alkalinisation of the media and ion release from the scaffold. pH change, ion release, and immunomodulatory properties of the scaffold could be modulated by the PLGA coating. Contrary to the hypothesis, the coating functioned by attenuating the BAG surface reactions and subsequent anti-inflammatory properties, rather than inducing an elevated inflammatory response compared to BAG-S53P4 alone. These results further validated the use of BAG-S53P4 (\pm PLGA) scaffolds as bone substitutes and indicate that scaffold properties can be tailored to a specific clinical need.

Keywords: Bioactive glass, S53P4, PLGA, anti-inflammatory, osteogenesis stimulation.

***Address for correspondence:** Robert Björkenheim, Department of Musculoskeletal and Plastic Surgery, University of Helsinki, Helsinki University Hospital, Topeliuksenkatu 5B, 3rd floor, 00260 Helsinki, Finland. Telephone number: +358 94711 Email: robert.bjorkenheim@hus.fi

Copyright policy: This article is distributed in accordance with Creative Commons Attribution Licence (<http://creativecommons.org/licenses/by-sa/4.0/>).

List of Abbreviations

ANOVA	analysis of variance	cDNA	complementary DNA
AR	alizarin red	EDX	electron-dispersive X-ray analysis
BAGs	bioactive glasses	ELISA	enzyme-linked-immunosorbent assays
BM	basal MSC growth medium	FMOD	fibromodulin
BMP	bone morphogenetic protein	GM-CSF	granulocyte macrophage colony-stimulating factor

HA	hydroxyapatite
h-PBMCs	human peripheral blood mononuclear cells
HPRT1	hypoxanthine phosphoribosyltransferase 1
ICP-OES	inductively-coupled-plasma-optical-emission spectrometry
IL-1Ra	interleukin-1 receptor antagonist
IL-1 β	interleukin 1 β
IL-6	interleukin 6
IM	induced membrane
IMT	induced membrane technique
LAL	<i>Limulus</i> amoebocyte lysate
LDH	lactate dehydrogenase
LPS	lipopolysaccharide
mRNA	messenger ribonucleic acid
MSC	mesenchymal stem cell
OGN	osteo glycin
OM	osteogenic differentiation medium
PBS	phosphate-buffered saline
PFA	paraformaldehyde
PLGA	poly(DL-lactide-co-glycolide)
qPCR	quantitative polymerase chain reaction
Rb-MSCs	rabbit bone marrow-derived MSCs
RPLP0	ribosomal protein lateral stalk subunit P0
RT-qPCR	reverse transcriptase quantitative polymerase chain reaction
RUNX2	runt-related transcription factor 2
SEM	scanning electron microscopy
SFM	serum-free medium
TNF α	tumour necrosis factor α
VEGF	vascular endothelial growth factor

Introduction

BAGs were first described by Hench and Paschall in the late 1960s (Hench and Paschall, 1973) and have since been a focus of increasing interest for biomedical applications. In particular, BAGs have emerged as effective bone graft substitutes that have both osteoconductive and osteostimulative properties (Hench *et al.*, 2000; Hench *et al.*, 2004; Wilson and Low, 1992; Xynos *et al.*, 2000; Xynos *et al.*, 2001). In the bone tissue microenvironment, a layer of HA is formed on the surface of the BAG that allows direct osteoconduction and formation of a strong mechanical bond between the material and bone. In addition, various dissolution products, such as Si, Ca, and P species released from silicate-based BAGs (SiO₂-CaO-Na₂O-P₂O₅) have been shown to stimulate osteogenic gene expression in cells involved in bone healing (Hoppe *et al.*, 2011).

BAG-S53P4 granules, a specific type of BAG, are widely used as a bone graft substitute for bone tumours, trauma, and spine surgery. Indeed, it has been stated that BAG-S53P4 is the most frequently used BAG in clinical practice (Baino *et al.*, 2018; Jones, 2013). In addition to promoting bone regeneration,

BAG-S53P4 granules have antimicrobial properties that are based on the elevation of pH in the local microenvironment, due to the dissolution of the BAG (Stoor *et al.*, 1998). Furthermore, the changes in osmotic pressure and ion concentrations have been reported to contribute to the antimicrobial properties (Leppäranta *et al.*, 2008; Munukka *et al.*, 2008; Zhang *et al.*, 2010). Thus, BAG-S53P4 granules are also used in the treatment of severe chronic osteomyelitis, mastoiditis as well as spine and frontal sinus infections (Kankare and Lindfors, 2016; Lindfors *et al.*, 2010a; Lindfors *et al.*, 2009; Lindfors *et al.*, 2010b; Stoor *et al.*, 2010).

IMT (Masquelet *et al.*, 2000) has emerged as an effective method for treating bone defects. At present, the IMT is a 2-staged procedure; first, a foreign body membrane is induced around the defect area by utilising a temporary spacer, followed by removal of the spacer and filling of the defect with a bone graft or corresponding substituent. The induced membrane, surrounding the defect and the bone graft, conveys ample vasculature. It also contains osteoprogenitor cells, and releases cytokines and growth factors (Gruber *et al.*, 2016) – *i.e.* several factors of the diamond (Giannoudis *et al.*, 2007) or hexagon (Loi *et al.*, 2016) concept required for successful bone healing. The induced membrane also contains high concentrations of VEGF and other growth factors essential for inducing vascularisation and bone formation (Pelissier *et al.*, 2004). The unique properties of the BAG, such as its osteoconductive, osteostimulative, and anti-microbial properties, would make the material ideal for the development of a 1-staged IMT. Indeed, an ongoing clinical trial (Tanner *et al.*, 2018) is investigating the use of BAG-S53P4 granules as the sole substitute in filling of segmental defects using the IMT.

A BAG-S53P4 scaffold was developed by sintering S53P4 granules. It was hypothesised that this scaffold could be used as the sole bone substitute to fill bone defects, with the additional ability of inducing a bioactive membrane around the bone defect site. Such an approach would convert the 2-stage IMT into a 1-stage technique, thus eliminating the need for additional surgery and potential complications related to the second procedure. Indeed, it has been shown, in an *in vivo* rabbit model, that sintered BAG-S53P4 scaffolds not only stimulate early bone formation within the scaffold, but also induce a bioactive membrane with ample microvasculature and upregulated VEGF and BMP expression (Björkenheim *et al.*, 2017; Björkenheim *et al.*, 2019). In addition to giving the sintered BAG scaffold increased mechanical strength (Mantsos *et al.*, 2009; Shi *et al.*, 2018), PLGA coating is hypothesised to induce a stronger initial inflammatory reaction than BAG-S53P4 alone, with enhanced induced membrane formation and bone regeneration (Björkenheim *et al.*, 2017; Björkenheim *et al.*, 2019; Nicolette *et al.*, 2011). This concept of polymer coated BAG scaffolds is not new; one of the first BAG scaffolds with

polymer coating was described by Chen *et al.* in 2006 (Chen and Boccaccini, 2006). Due to brittleness, the 4S55 scaffolds were coated with the polymer poly(D,L-lactic acid) to achieve enhanced mechanical properties (Chen and Boccaccini, 2006). Furthermore, BAG in combination with PLGA can evoke enhanced biological activities both *in vitro* and *in vivo*, compared to BAG alone (Magri *et al.*, 2019).

The aim of this study was to characterise the various cell biological effects of BAG-S53P4 scaffolds and the effects of PLGA coating for use in a single-stage IMT (Masquelet, 2000). Both the immunomodulatory and osteogenic properties of the scaffolds in macrophage and MSC culture models, respectively, were assessed. The pH change and ions released by dissolving scaffolds were also assessed in order to understand the underlying cellular biological mechanisms.

Materials and Methods

Production and coating of bioactive glass scaffolds

BAG-S53P4 (\pm PLGA) scaffolds were manufactured as previously described (Björkenheim *et al.*, 2017; Björkenheim *et al.*, 2019). Briefly, BAG-S53P4 (composition in wt%: 53 % SiO₂, 23 % NaO, 20 % CaO and 4 % P₂O₅) was first melted and then cast into a graphite mould. After annealing, the glass was crushed, sieved into 300 to 500 μ m granules and sintered into cylinder shapes using a graphite mould at 720 °C for 90 min. The final dimensions of the scaffolds were 5 \times 15 mm. Designated BAG scaffolds were dip coated with an acid-terminated PLGA called PDLG5002A at a 50 : 50 ratio between DL-lactide and glycolide (Corbion, Gorinchem, the Netherlands). The theoretical minimum degradation time of the utilised PLGA is 14 d (Cyphert *et al.*, 2020). After coating, the BAG-S53P4-PLGA scaffolds were dried in air and vacuum. All scaffolds were sterilised by gamma irradiation with a dose of 25 kGy. The average mass of the scaffolds was 351.9 \pm 13.6 mg and the average mass of the coating for selected scaffolds was 35.0 \pm 4.7 mg. For cell stimulations, scaffolds were randomised to minimise possible effects of variability in glass scaffold and coating mass.

Cell culture and stimulation with intact scaffolds

Monocyte isolation and differentiation

h-PBMCs were isolated from buffy coats of healthy volunteer blood donors who provided signed informed consent. Buffy coats were by-products of blood preparation for clinical purposes, and their use for monocyte isolation was approved by the Finnish Red Cross Blood Service. The donors were 2 men and 2 women with a mean age of 39 years; the reported data include analysis from all four specimens ($n = 4$). Mononuclear cells were isolated and differentiated into macrophages, following a

previously described protocol (Nurmi *et al.*, 2017). Briefly, blood samples were diluted in Ca/Mg-free PBS, carefully added on top of a Ficoll-Paque PLUS density gradient medium (Supplier, city, state, country), and centrifuged at 800 $\times g$ for 30 min. The mononuclear cell layer was collected and washed 4 times with PBS. Freshly isolated monocytes were then suspended in Dulbecco's modified Eagle's medium (Sigma-Aldrich, Saint Louis, MO, USA) supplemented with 1 % penicillin-streptomycin antibiotic solution (Gibco, Life Technologies, Grand Island, NY, USA), counted using a TC20 automated cell counter (Bio-Rad, Hercules, CA, USA), and plated onto 24-well culture plates (well surface area 1.9 cm²) (Greiner Cellstar, Kremsmünster, Austria) at a concentration of 1.5 $\times 10^6$ cells/well. Cells were allowed to adhere for 1 h in a humidified 37 °C incubator at 5 % CO₂ and were then rinsed twice with PBS to remove non-adherent cells. Adherent monocytes were differentiated into macrophages during a 7 d culture in macrophage SFM (Gibco), supplemented with 100 U/mL penicillin, 100 μ g/mL streptomycin, and 10 ng/mL GM-CSF (Miltenyi Biotec, Bergisch Gladbach, Germany).

Macrophage stimulation with scaffolds

To study the inflammatory response indirectly induced by BAG-S53P4 (\pm PLGA), scaffolds were introduced to macrophage cultures 1 scaffold/well and incubated for 6 or 24 h. At a given timepoint, scaffolds were removed from the wells, culture supernatants were collected, and cells disrupted by adding RLT Plus lysis buffer (Qiagen, Valencia, CA, USA). Culture media and cell lysates were stored at -75 °C for later use. To study the indirect immunomodulatory effect of BAGs, BAG-S53P4 and BAG-S53P4-PLGA scaffolds were introduced to the wells on day 6 of macrophage culturing, thereby allowing the scaffolds to interact with cells for 24 h. On day 7, culture media were further supplemented with 100 ng/mL LPS (Sigma-Aldrich) for either 6 or 24 h. At both timepoints, cell lysates and media samples were obtained as described above. LPS concentration was chosen based on a previous investigation (Day and Boccaccini, 2005). All stimulations were performed in duplicate wells, with appropriate controls included. Cell lysates from the 6 h timepoint were directed to qPCR analysis, whereas media samples from the 24 h stimulation were analysed using ELISA. Cell viability was measured from the culture media using an LDH detection kit (Roche Diagnostics, Basel, Switzerland) according to the manufacturer's instructions.

ELISA

Concentrations of the cytokines TNF α , IL-1 β , IL-6 and IL-1Ra were analysed from 24 h macrophage culture media using sandwich ELISA (DuoSet kits, R&D Systems, Minneapolis, MN), according to the manufacturer's instructions. The pro-inflammatory cytokines TNF α , IL-1 β , and IL-6 are central for

initiating the fracture repair (bone regeneration) cascade (Einhorn *et al.*, 1995; Gerstenfeld *et al.*, 2003; Lange *et al.*, 2010). The initial inflammatory response to these factors includes recruitment of inflammatory and other cells necessary for bone regeneration and promotion of angiogenesis (Barnes *et al.*, 1999). IL-1Ra regulates the effects of IL-1 β and is regarded as an anti-inflammatory cytokine (Arend *et al.*, 1998).

Evaluation of LPS binding to scaffold

Possible LPS binding to BAG-S53P4 (\pm PLGA) scaffolds was explored by simulating the macrophage-stimulation experiment on a 24-well plate (well surface area 1.9 cm²) (Cellstar). BAG-S53P4 and BAG-S53P4-PLGA scaffolds were immersed in complete macrophage culture medium and incubated for 24 h in a 37 °C incubator. Thereafter, media were supplemented with 100 ng/mL of LPS and incubated for an additional 6 or 24 h. Medium without a scaffold served as a positive control. LPS levels were determined from these media following the manufacturer's protocol using a LAL quantitation kit (Pierce LAL Chromogenic Endotoxin Quantitation Kit, Thermo Scientific, Waltham, MA, USA) and serial dilutions of endotoxin standards.

Rb-MSCs stimulation

To study the indirect osteogenic properties of BAG-S53P4 (\pm PLGA) scaffolds, Rb-MSCs (Cat. No. RBXMX-01001, Oricell, Cyagen Biosciences Inc., CA, USA) in phase P4 were cultured on a 12-well culture plate (well surface area 3.9 cm²) (Cellstar) in Oricell BM (Cat. Nr. GUXMX-90011, Cyagen Biosciences

Inc.) with a cell count of 1.2×10^4 cells/well. Rb-MSCs were selected because rabbit *in vivo* models were used in past experiments. Furthermore, these cells have been shown to closely resemble human MSCs in osteogenesis experiments (Tan *et al.*, 2013; Zomer *et al.*, 2018). The culture plates were coated with 0.1 % porcine gelatine (Immunoassay grade gelatine, product nr. 1706537, Bio Rad, USA) prior to seeding and cells were allowed to reach 70 % to 80 % confluence before the start of the experiment. The scaffolds were immersed in wells with the MSCs in a total medium volume of 2 mL. Oricell MSC OM (Cat. Nr. GUXMX-90021, Cyagen Biosciences Inc.) and Oricell MSC growth medium without scaffolds were used as positive and negative controls, respectively. Cells were refreshed every 3 d until the end of the experiment at 11 d, at which point mineralisation was assessed. This early timepoint (11 d) for mineralisation assessment was chosen based on a pilot study, where mineralisation was seen in the control cells after 14 d of stimulation. The aim was to demonstrate that mineralisation occurs earlier in scaffold-stimulated cells than in control cells and to possibly evaluate the differences between the non-coated and coated BAG-S53P4 scaffolds. To exclude the possibility of mineralisation due to mineral precipitation from BAG on the cell culture plate surface, an identical mineralisation experiment was conducted without cells present. In addition, cell lysate samples were collected at 3 and 7 d timepoints. These experiments, with or without Rb-MSCs, were repeated independently 3 times ($n = 3$). Cell media samples from 1 experiment ($n = 1$) were collected at

Table 1. Primer sequences used for qPCR analysis of human macrophages.

Gene	Primer	Primer sequence (5'-3')
TNF α	Forward	TGCTGCACTTTGGAGTGATCG
	Reverse	ATCTCTCAGCTCCACGCCATT
IL-1 β	Forward	TGGCAATGAGGATGACTTGT
	Reverse	GGAAAGAAGGTGCTCAGGTC
RPLP0	Forward	GAAATCCTGAGTGATGTGCAGC
	Reverse	TCGAACACCTGCTGGATGAC

Table 2. Primer sequences used for qPCR analysis of Rb-MSCs.

Gene	Primer	Primer sequence (5'-3')	Acc no.	Product
RUNX2	Forward	TCTGGCCTTCCACTCTCAGT	AY598934.1	127 bp
	Reverse	TGCATTCGTGGGTTGGAGAA		
FMOD	Forward	ATCCTGCTGGACCTGAGCTA	AF020291	104 bp
	Reverse	GGGACGGTGTAGACGTTGTT		
OGN	Forward	CTGCCAGAAAGTTTGCCTG	AF487889	129 bp
	Reverse	GCCCTCCAGCCGTATTTCTT		
HPRT1	Forward	ACGTCGAGGACTTGGAAAGG	NM_001105671	111 bp
	Reverse	GGGCTACAATGTGATGGCCT		

6 h, 1 d, 3 d, 7 d and 11 d timepoints for ICP-OES analysis.

RT-qPCR

Total RNA was extracted and purified from macrophage and Rb-MSC lysates using an RNeasy Mini Kit (Qiagen) according to the manufacturer's protocol. The amount of RNA was measured using a NanoDrop™ 1000 spectrophotometer (Thermo Scientific) and 100 ng of isolated RNA from each sample was reverse transcribed into cDNA using an iScript cDNA synthesis kit (Bio-Rad). Quantitative real-time PCR was performed in a LightCycler instrument (Roche) in duplicate wells. The qPCR reaction mix consisted of HOT FIREPol EvaGreen qPCR SuperMix reagent (Solis BioDyne, Tartu, Estonia), 20 ng of sample cDNA, and primer mix (forward and reverse primers). For negative controls, the cDNA sample volume was substituted with RNase-free water.

To evaluate the inflammatory response of human macrophages to BAG-S53P4 (\pm PLGA) scaffolds, the relative expressions of *TNF α* and *IL-1 β* were analysed at the 6 h timepoint. NCBI/Primer-BLAST was used to design PCR primers (Table 1). The results were normalised to the housekeeping gene *RPLP0*.

To measure the osteogenic differentiation response of Rb-MSCs to BAG-S53P4 (\pm PLGA) scaffolds, the relative expression of *RUNX2*, *FMOD*, and *OGN* were analysed at the 3 and 7 d timepoints. Primers for these genes are listed in Table 2. Results were normalised to the housekeeping gene *HPRT1*.

Mineralisation assay

The mineralisation assay was conducted on Rb-MSCs after the 11 d stimulation with BAG-S53P4 (\pm PLGA) scaffolds. Quantitative measurement of mineralisation was evaluated with OsteoImage™ mineralisation assay (Lonza, Basel, Switzerland). The assay was conducted according to the manufacturer's instructions. Briefly, following removal of media, Rb-MSCs were fixed with 4 % PFA for 30 min and incubated with staining solution for 30 min at room temperature. The quantitative fluorescence was measured at 480/520 nm excitation/emission wavelengths (Hidex, Turku, Finland / Spark, Tecan Trading AG, Männedorf, Switzerland). Due to critical equipment failure, 2 different fluorescence readers were used in the study and a correction factor was calculated to harmonise the results between the readers.

AR stain

Mineralisation of BAG-S53P4 (\pm PLGA) scaffold-stimulated Rb-MSC cultures and mineralisation of control wells without cells were assessed qualitatively at the 11 d timepoint by staining the calcium deposits with AR (Cyagen Biosciences Inc.). Cells were fixed with 4 % PFA for 30 min and stained with AR solution for 5 min at room temperature. Control wells without

cells were also incubated in 4 % PFA to produce similar conditions to the experiment performed with cells. After washing with PBS, the wells images of the cells were captured. AR staining identifies calcium deposits while OsteoImage™ binds to HA and thus these 2 methods of determining bone formation were complementary to each other.

ICP-OES

The concentrations of the elements Si, Ca and P were analysed from the culture medium of Rb-MSCs incubated with BAG-S53P4 (\pm PLGA) scaffolds using ICP-OES (Optima 5300 DV; Perkin Elmer, Waltham, MA, USA).

SEM and EDX

BAG-S53P4 (\pm PLGA) scaffolds, used in Rb-MSCs stimulation, were collected and analysed by SEM and EDX after 11 d of immersion in Oricell MSC growth medium. The reaction layers that formed on the scaffold surfaces were viewed using a Leo Gemini 1530 SEM instrument equipped for electron-dispersive X-ray analysis (Carl Zeiss, Oberkochen, Germany / EDX Thermo Electron Company). The scaffold cross-sections were imaged from scaffolds that had been cast to epoxy, cut to reveal the cross-sections, and then polished using SiC papers before the analysis.

pH measurements

The pH measurements of cell culture media (macrophage-SFM and Oricell Rb-MSC basal growth medium) with and without the presence of BAG-S53P4 (\pm PLGA) scaffolds in a 12-well cell culture plate (Cellstar) were conducted using a Thermo Scientific™ Orion™ PerpHecT™ ROSS™ Combination pH Micro Electrode (Thermo Scientific). The experiment was performed without the presence of cells but otherwise in an identical setting compared with the above-mentioned experiments with macrophages and Rb-MSCs. The pH was measured at baseline (*i.e.* before scaffold introduction) and at 15 min, 30 min, 1 h, 6 h and 1 d in both media and additionally at 3 d, 7 d and 11 d timepoints for the Oricell Rb-MSC basal growth medium. The measurements were taken from triplicate wells ($n = 3$).

Statistical analyses

Statistical analyses were performed using GraphPad Prism version 8 (GraphPad Software, La Jolla, CA, USA). The experiments with human primary macrophages ($n = 4$) were analysed using Friedman's test and Dunn's multiple comparison tests. For other experiments, consisting of three parallel samples ($n = 3$), statistical comparison between groups was conducted by one-way ANOVA followed by Holm-Sidak's *post-hoc* tests. $p < 0.05$ was chosen as the threshold for statistical significance. Results are presented as mean \pm standard error of mean.

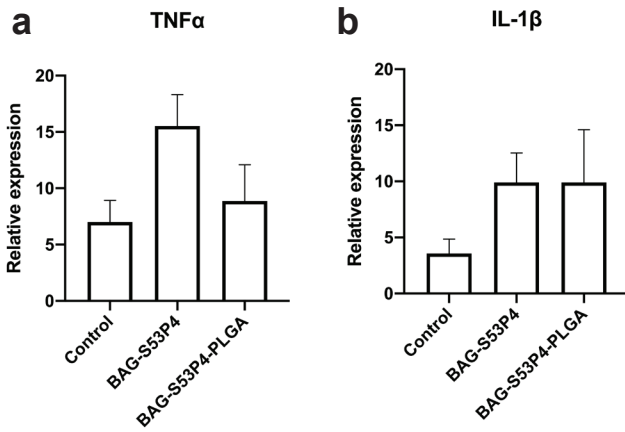


Fig. 1. Scaffold stimulation of macrophages without LPS treatment. Human primary macrophages were stimulated with BAG-S53P4 (\pm PLGA) scaffolds for 6 and 24 h and the inflammatory response was assessed by qPCR and ELISA. Relative mRNA expression of (a) TNF α and (b) IL-1 β were determined after 6 h of scaffold stimulation, whereas cytokine secretion for (c) TNF α , (d) IL-1 β , (e) IL-6, and (f) IL-1Ra were measured at the 24 h timepoint (* = $p < 0.05$).

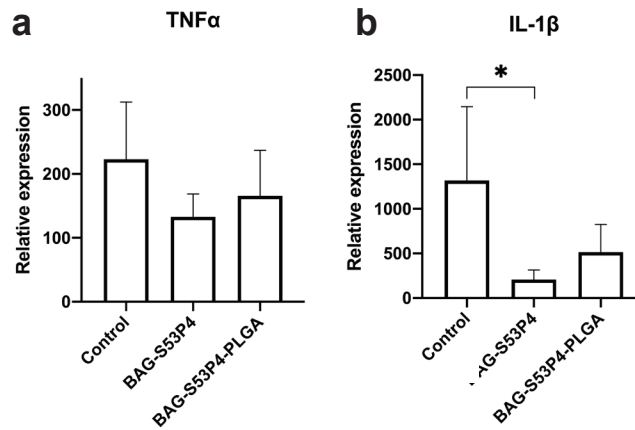
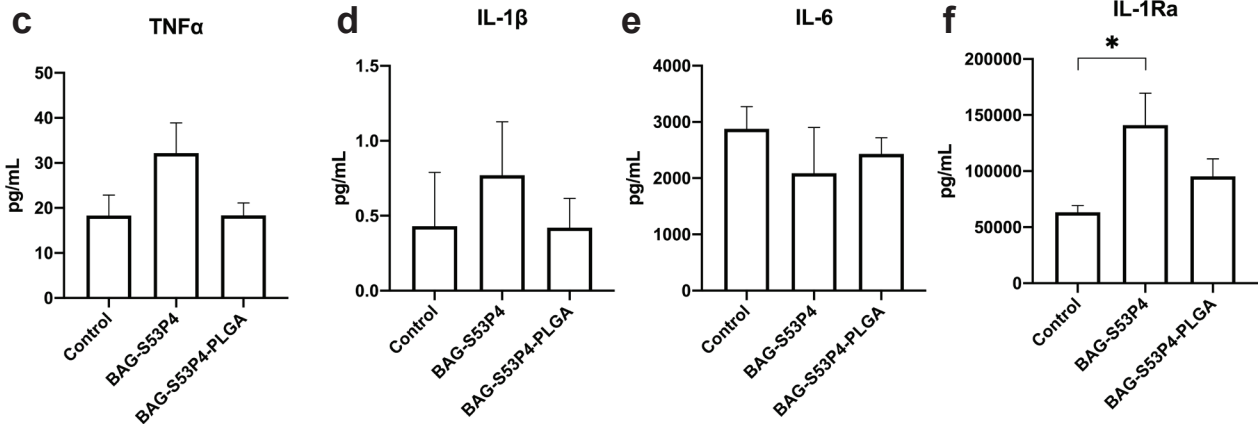
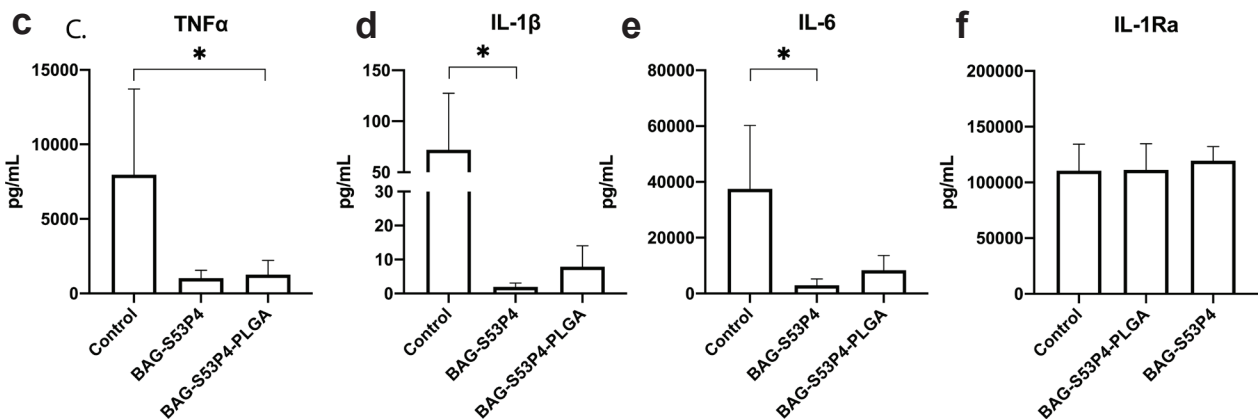


Fig. 2. Immunomodulatory effect of scaffolds on LPS-challenged macrophages. Human primary macrophages were preincubated with BAG-S53P4 (\pm PLGA) scaffolds for 24 h, after which the culture media were further supplemented with LPS for 6 or 24 h. The relative mRNA expression of (a) TNF α and (b) IL-1 β were determined by qPCR after 6 h of LPS stimulation. Secretion of pro-inflammatory cytokines (c) TNF α , (d) IL-1 β , and (e) IL-6 and anti-inflammatory cytokine (f) IL-1Ra were assessed, following a 24 h LPS challenge, using ELISA (* = $p < 0.05$).



Results

Inflammatory reaction to scaffolds *in vitro*

The potential inflammatory reaction, elicited by BAG-S53P4 (\pm PLGA) scaffolds, was evaluated in a human macrophage culture model. Introduction of BAG-S53P4 (\pm PLGA) scaffolds to macrophages did not induce the expression of TNF α or IL-1 β mRNA at the 6 h timepoint, as analysed by qPCR (Fig. 1a,b). Similarly, macrophages challenged with BAG-S53P4 (\pm PLGA) scaffolds for 24 h did not elicit significant production of the pro-inflammatory cytokines TNF α , IL-1 β and IL-6, as assessed by ELISA (Fig. 1c-e). In contrast, secretion of the anti-inflammatory cytokine IL-1Ra was elevated at 24 h by BAG-S53P4 (\pm PLGA) scaffolds; the non-coated BAG-S53P4 exhibited significantly higher IL-1Ra production compared with control samples (Fig. 1f). However, the difference in IL-1Ra concentrations between BAG-S53P4 and BAG-S53P4-PLGA was not significant.

Anti-inflammatory effects of scaffolds *in vitro*

The immunomodulatory properties of the BAG-S53P4 (\pm PLGA) scaffolds were assessed using cultured human macrophages challenged with LPS. As expected, LPS stimulation markedly upregulated the mRNA expression of TNF α and IL-1 β after 6 h, as assessed by qPCR (Fig. 2a,b). Similarly, LPS-challenged macrophages exhibited markedly elevated secretion of the pro-inflammatory cytokines TNF α , IL-1 β and IL-6 at 24 h, as assessed by ELISA.

Interestingly, preincubation of macrophages with BAG-S53P4 (\pm PLGA) scaffolds, prior to and during the LPS challenge, seemed to lower the relative mRNA expressions of TNF α and IL-1 β when compared with cells stimulated with LPS alone (Fig. 2a,b). This reduction in IL-1 β expression was statistically significant for BAG-S53P4-treated macrophages (Fig. 2b). A similar trend was observed when analysing the secretion of TNF α , IL-1 β and IL-6; macrophages stimulated with LPS in combination with the BAG-S53P4 (\pm PLGA) scaffolds exhibited decreased secretion of these pro-inflammatory cytokines (Fig. 2c-e). LPS-challenged macrophages incubated with BAG-S53P4 (\pm PLGA) scaffolds showed no difference in TNF α secretion. However, a statistically significant difference was noted for BAG-S53P4-PLGA when compared with control cells (Fig. 2c). PLGA coating, however, marginally elevated IL-1 β and IL-6 concentrations when compared with the non-coated BAG-S53P4 scaffold (Fig. 2d-e). Although clear trends were seen in the pro-inflammatory immunomodulation of BAG-S53P4 (\pm PLGA) scaffolds on LPS-challenged human macrophages, only a few statistically significant differences were observed, due to high donor variability between the 4 donors. The concentration of the anti-inflammatory cytokine IL-1Ra remained unaffected by BAG-S53P4 (\pm PLGA) scaffold stimulation as compared with control cells (Fig. 2f).

To determine if the observed immunomodulatory effects could be artefacts due to cytotoxicity or non-specific binding of LPS on the porous scaffold, cell viability and the LPS recovery rates after scaffold incubations were assessed. The scaffold-induced

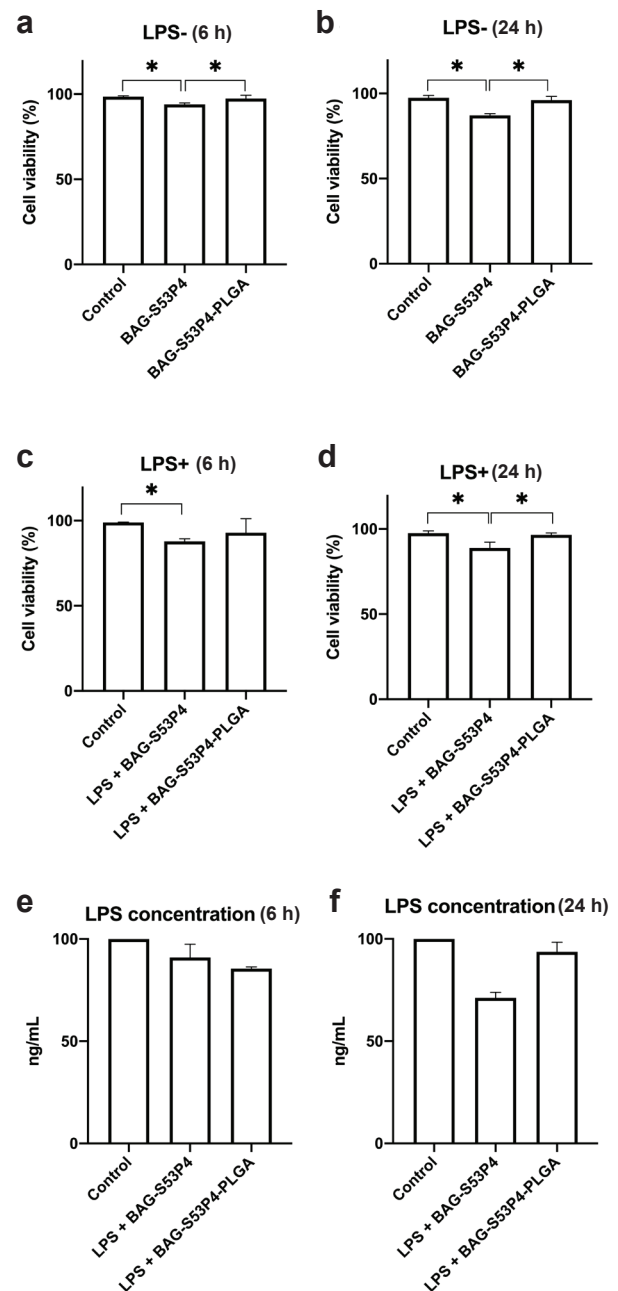


Fig. 3. Cell viability of macrophages and LPS binding to the scaffold. Human primary macrophages were incubated in the presence of BAG-S53P4 (\pm PLGA) scaffolds and scaffold-induced cytotoxicity was determined at (a) 6 h and (b) 24 h timepoints using an LDH assay. The combined effects of scaffold preincubation and subsequent LPS challenge on cell viability were analysed after (c) 6 and (d) 24 h of LPS treatment. Binding of LPS to the surface of preincubated scaffolds was assessed using a LAL assay after (e) 6 h and (f) 24 h of LPS stimulation. * indicates statistically significant difference between conditions (* = $p < 0.05$).

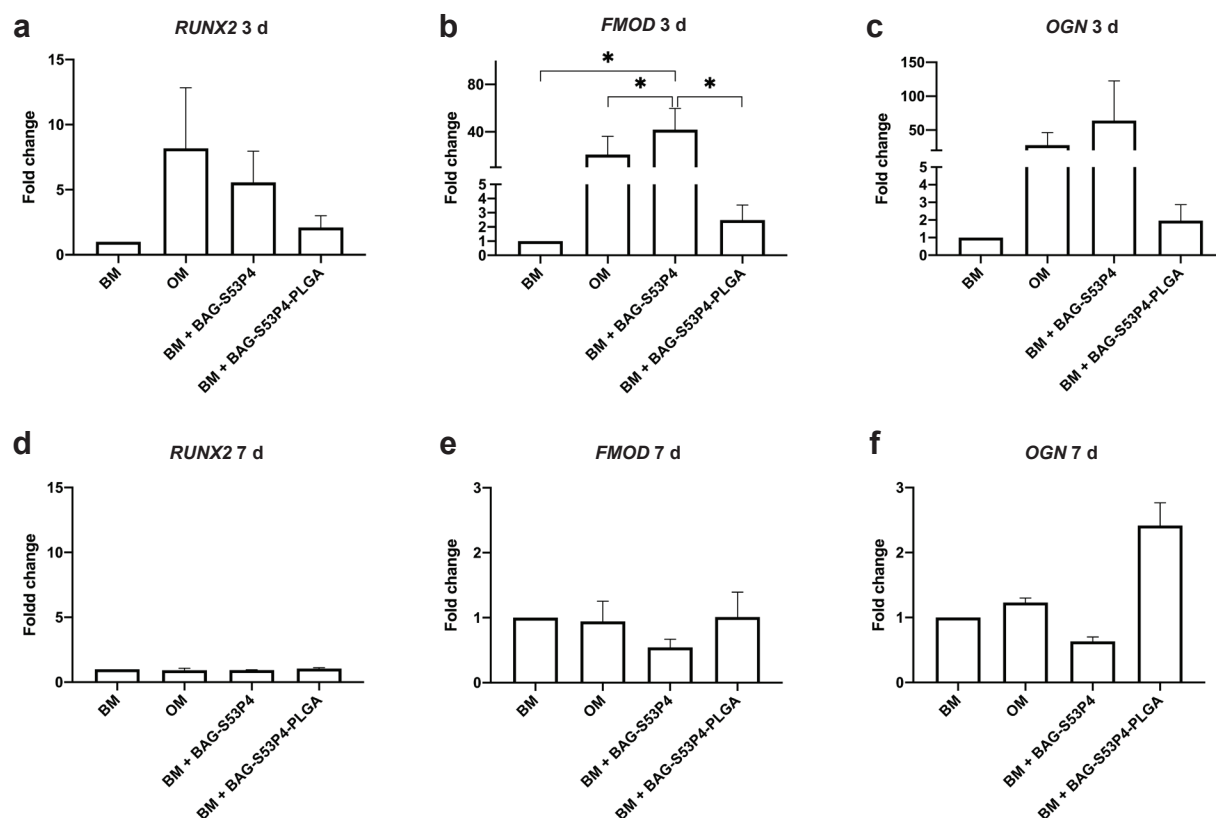


Fig. 4. Relative mRNA expression of osteogenic markers. Rb-MSCs were cultured in the presence of BAG-S53P4 (\pm PLGA) scaffolds and their relative mRNA expression of *RUNX2*, *FMOD* and *OGN* was analysed after (a-c) 3 and (d-f) 7 d. Cells cultured in osteogenic differentiation medium (OM) served as a positive control. Results are presented as fold change compared with unstimulated control cells cultured in basal MSC growth medium (BM) (* = $p < 0.05$).

cytotoxicity in human macrophage cultures was evaluated by measuring LDH release. Compared with controls, a modest decrease in cell viability was observed in the scaffold groups (Fig. 3a,b). This effect was slightly enhanced by the addition of LPS (Fig. 3c,d). BAG-S53P4 scaffolds induced higher cytotoxicity when compared with control and BAG-S53P4-PLGA groups.

Some LPS binding occurred on the scaffold surfaces, as slightly reduced LPS amounts were recovered from the media of the scaffold groups after 6 and 24 h culture (Fig. 3e,f). These differences, however, were not statistically significant.

Induction of osteogenesis in rabbit MSC cultures

As analysed by qPCR, Rb-MSCs stimulated with BAG-S53P4 scaffolds showed elevated mRNA expression of osteogenic markers *RUNX2*, *FMOD*, and *OGN* after 3 d of culturing (Fig. 4a-c). Of these changes, the increase in *FMOD* expression reached statistical significance (Fig. 4b). A similar response profile was observed for cells cultured in OM. In contrast, PLGA-coated scaffolds induced low mRNA levels of these markers at the 3 d timepoint. After 7 d, the mRNA expression of *RUNX2*, *FMOD*, and *OGN* in OM cells and BAG-S53P4 (\pm PLGA) cells had returned to the level of unstimulated control cells cultured in basal MSC growth medium (BM)

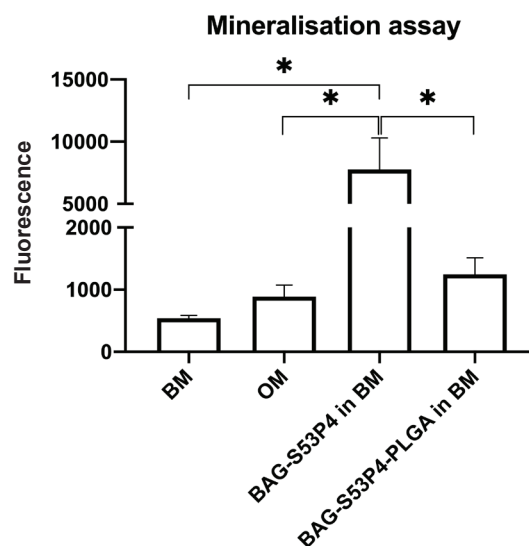


Fig. 5. Scaffold-induced mineralisation measured using OsteoImage™ assay. Rb-MSCs were cultured in the presence of BAG-S53P4 (\pm PLGA) scaffolds for 11 d and culture mineralisation was assessed using an OsteoImage™ assay. Cells in osteogenic differentiation medium (OM) and basal MSC growth medium (BM) served as controls. * indicates statistically significant difference between conditions (* = $p < 0.05$).

(Fig. 4d-f). Interestingly, Rb-MSCs stimulated with BAG-S53P4-PLGA scaffolds still maintained slightly increased, but not statistically significant, *OGN* expression after 7 d (Fig. 4f). This might be due to the PLGA coating, which delays and subdues the effects of the underlying BAG.

Mineralisation of the Rb-MSC cultures was assessed at the 11 d timepoint. Quantitative measurements showed that cells stimulated with BAG-S53P4 scaffolds had significantly increased mineralisation compared with all other groups (Fig. 5). Rb-MSCs stimulated with BAG-S53P4-PLGA scaffolds and cells cultured in OM induced similar levels of mineralisation; both were marginally higher than unstimulated control cells. The minimal mineralisation of OM-cultured Rb-MSCs was probably due to the shortened 11 d stimulation time. Corresponding mineralisation patterns were evident in qualitative AR staining (Fig. 6a-d). Of note, some

calcium deposition also occurred on the bottom of the well in BM without cells, incubated with BAG-S53P4 scaffolds. This mineralisation, probably due to surface precipitation of Ca and P ions dissolved from scaffold, was only seen at the site of direct scaffold contact with the cell culture well (Fig. 6e-h). In contrast, in the experiments containing Rb-MSCs, the mineralisation was evident over a wider surface area, also at sites where scaffolds were not in direct contact with the well surface. Thus, although it can be concluded that the BAG-S53P4 scaffolds stimulate mineralisation in Rb-MSC, the quantitative measurements must be interpreted with caution due to evident mineralisation of the scaffold itself.

Ion release into the cell culture media

Ion release from the BAG-S53P4 (\pm PLGA) scaffolds in cell culture conditions was assessed using ICP-OES, in a time-course study. The Si species concentration

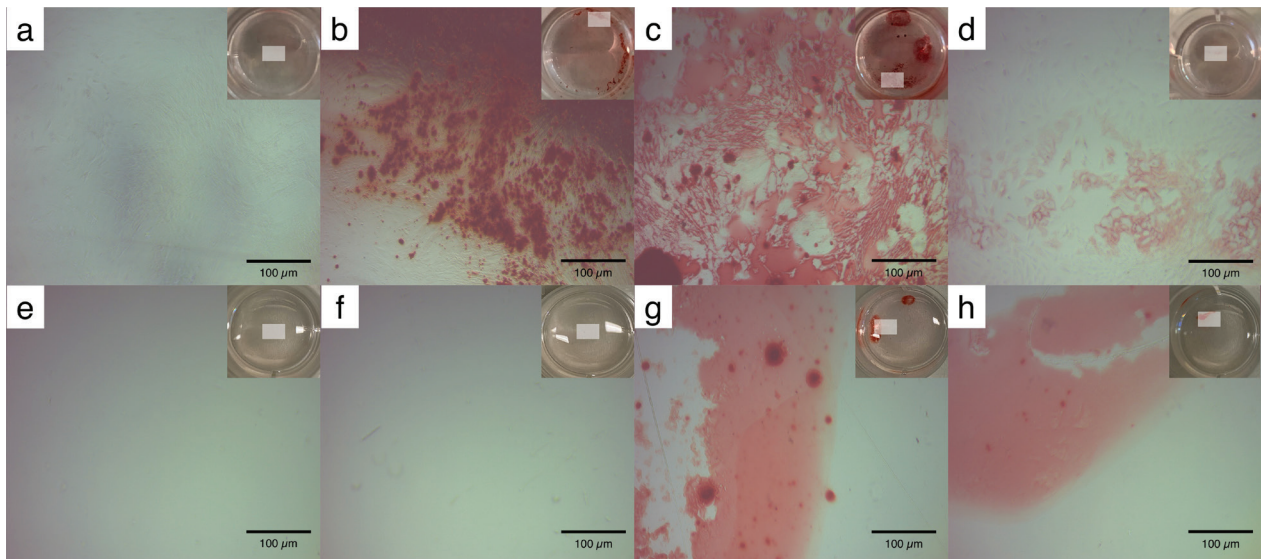


Fig. 6. Alizarin red staining. Rb-MSCs were cultured with BAG-S53P4 (\pm PLGA) scaffolds for 11 d and mineralisation was assessed by AR staining. Microscopy images of representative samples are shown for (a) unstimulated control cells in basal growth media (BM), (b) cells in osteogenic differentiation medium (OM), (c) BAG-S53P4-stimulated cells, (d) BAG-S53P4-PLGA-stimulated cells, (e) BM without cells, (f) OM without cells, (g) BM stimulated with BAG-S53P4 without cells and (h) BM stimulated with BAG-S53P4-PLGA without cells. Images of respective wells are embedded in the upper right corner of each micrograph and a rectangle marks the area of the microscopy image.

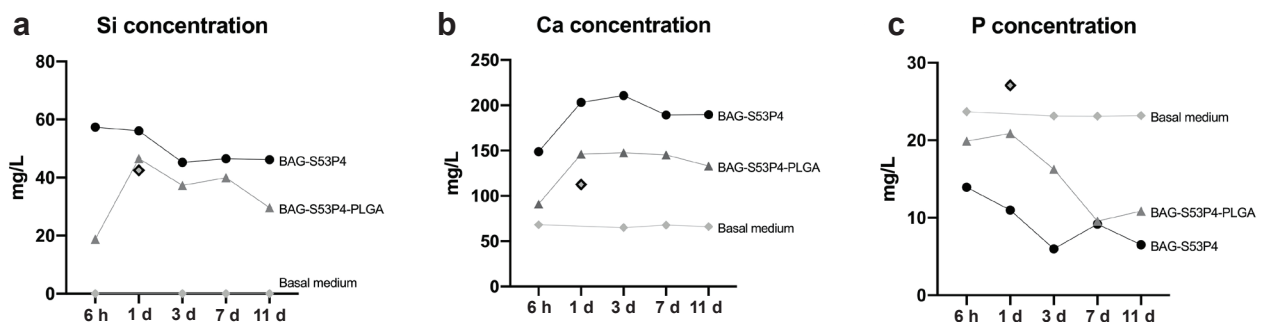


Fig. 7. Ion release from scaffolds ($n = 1$). BAG-S53P4 (\pm PLGA) scaffolds were immersed in Rb-MSC cultures and the media concentration for (a) Si, (b) Ca, and (c) P was measured after a 6 h, 1 d, 3 d, 7 d and 11 d incubation time by ICP-OES. Ions in basal MSC growth medium without a scaffold were included as reference values. The 1 d timepoint for basal medium control was rejected because of technical error in measurement.

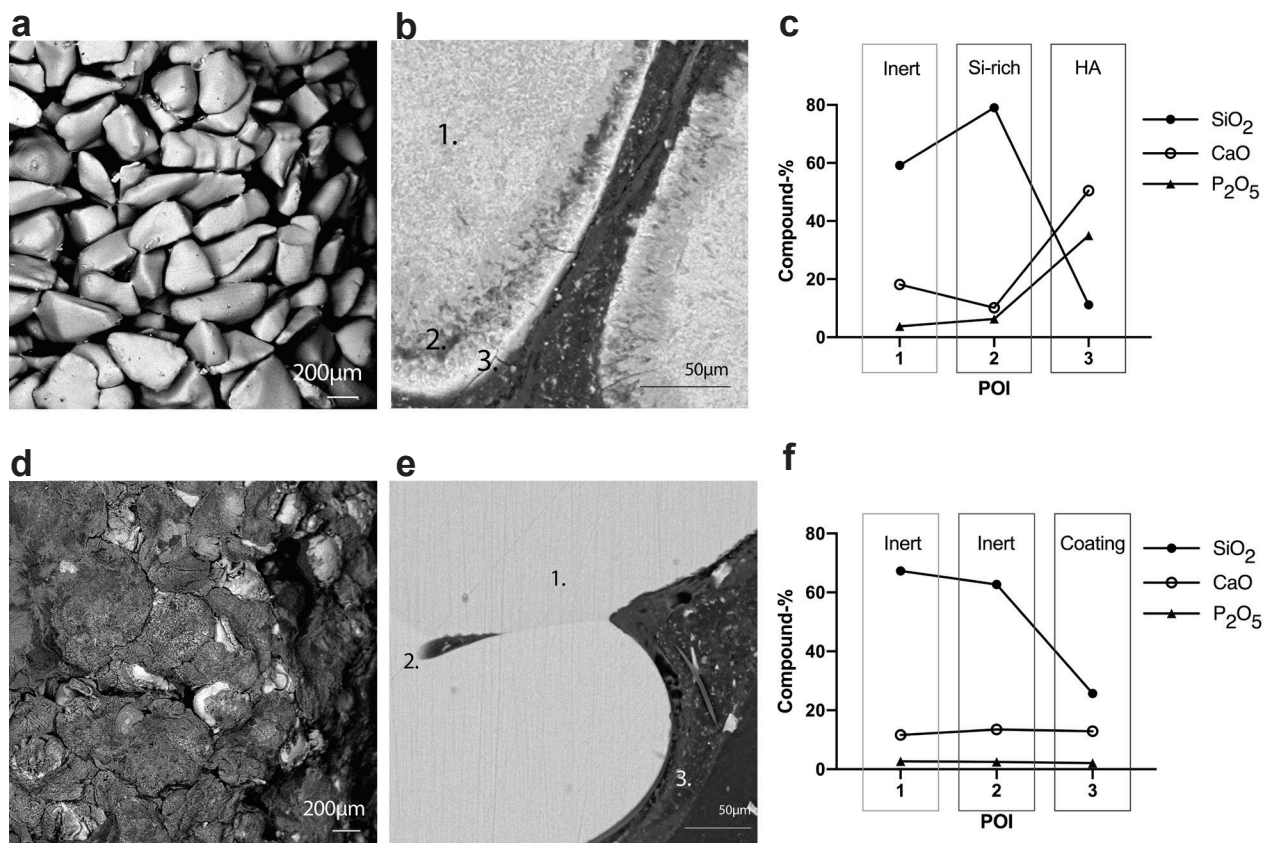


Fig. 8. SEM and EDX. SEM and EDX results of BAG-S53P4 (a-c) and BAG-S53P4-PLGA (d-f) scaffolds incubated in Rb-MSC cultures for 11 d. Representative images are presented for non-coated scaffolds (a), their cross-sectional surface where the reaction layer is visualised (b) and the EDX results from 3 different points of interest (POI) (c). EDX measurements reveal inert BAG in the middle, a silica-rich layer and an outer layer of CaP (c). Representative images are presented for coated scaffolds (d), their cross-sectional surface with no clear formations of reaction layers (e) confirmed by EDX analysis (f). Inert BAG is seen at 2 different POI and the outermost layer represents the coating material (f). Scalebars are located in the bottom right corners of respective images.

was the highest at the 6 h timepoint for BAG-S53P4 and showed a decrease at the 3 d timepoint, after which stable concentrations were measured (range 57 to 45 mg/L). BAG-S53P4-PLGA showed a Si peak at the 1 d timepoint, after which stabilisation occurred (range 19 to 47 mg/L). As expected, Si concentrations were not detectable in the control basal media sample because the basal cell media does not contain any Si species. Due to a technical error, the 1 d Si measurement timepoint for basal medium without scaffold was discarded (Fig. 7a).

For both coated and non-coated BAG-S53P4 scaffolds, the concentration of Ca ions increased until the 1 d timepoint, after which the concentration stabilised. At the 1 d timepoint, the Ca concentration was higher for BAG-S53P4 compared with BAG-S53P4-PLGA (203 *vs.* 146 mg/L). The Ca concentration in the basal medium alone was steady throughout the measurement period and varied from 65 to 68 mg/L (Fig. 7b).

The concentration of P species was highest at the 6 h timepoint and then declined until stabilisation after the 3 d timepoint. The decline was more rapid for the BAG-S53P4 scaffold, which reached a steady state at the 3 d timepoint, compared with the 7 d

timepoint for the BAG-S53P4-PLGA scaffold. Overall, the concentration of P species was lower for the non-coated BAG-S53P4 (range 14 to 6 mg/L) compared with coated BAG-S53P4-PLGA (range 21 to 9 mg/L). In control basal media, the P concentration was stable during the entire measurement period (range 24 to 23 mg/L) (Fig. 7c).

Deposition of calcium phosphate on scaffold surfaces

SEM images were taken from the surface of intact BAG-S53P4 (\pm PLGA) scaffolds incubated in Rb-MSC cultures for 11 d and reaction layers were identified by EDX analysis. Formation of a calcium and phosphate-rich (CaP) layer was observed on the surface of uncoated scaffolds by cross-sectional analysis, which confirmed the EDX analysis, revealing the reaction layer on the outermost BAG particles (Fig. 8a-c). EDX analysis from three different points of interest (POI) show inert BAG in the inner part of a granule, a silica-rich layer and a outermost CaP layer (Fig. 8c). Imaging of the coated scaffolds revealed that the PLGA coating was not entirely uniform and areas of uncoated particles were present (Fig. 8e). There was markedly less layer formation on

the surface of the PLGA-coated scaffolds and upon EDX analysis no clear layers could be identified (Fig. 8e,f). The formation of the reaction layer containing CaP is consistent with previous reports characterising the surface reactions of BAG-S53P4 (Fagerlund *et al.*, 2012).

pH of culture media

The baseline pH average from triplicate wells was 7.50 ± 0.01 in the macrophage-SFM and 7.34 ± 0.02 in the BM. A peak in pH was noted at the 30 min timepoint for all samples, after which the pH stabilised (Fig. 9a,b). Of note, the pH value of BAG-S53P4-PLGA in BM decreased at the 11 d timepoint. This might be due to continued PLGA degradation (Fig. 9b).

BAG-S53P4 significantly increased the pH at all timepoints compared with BAG-S53P4-PLGA and all control samples (Fig. 9a,b). BAG-S53P4-PLGA showed significant increases in pH values compared with macrophage-SFM and BM media control samples at the 15 min to 7 d timepoints. However, at the 11 d timepoint, the pH value of BAG-S53P4-PLGA in BM was significantly lower than control BM (Fig. 9a,b).

Discussion

In this study, the immunomodulatory and osteogenic properties of sintered BAG-S53P4 (\pm PLGA) scaffolds were assessed in human macrophage and rabbit MSC culture models, respectively. When placed in human macrophage cultures, the BAG-S53P4 scaffolds alone did not induce a significant inflammatory reaction, as assessed by production of the pro-inflammatory cytokines TNF α , IL-1 β and IL-6. Instead, the production of the anti-inflammatory cytokine IL-1Ra was upregulated in scaffold-challenged macrophage cultures, possibly suggesting that the non-coated BAG scaffolds have anti-inflammatory properties. The PLGA coating was also found not to induce an inflammatory response, as the production of TNF α , IL-1 β and IL-6 remained low in the BAG-S53P4-PLGA-challenged macrophage cultures. The production of IL-1Ra, however, was attenuated by PLGA coating. In LPS-stimulated macrophages, both TNF α and IL-1 β gene expression levels decreased when cells were first introduced to BAG-S53P4 (\pm PLGA) scaffolds. This anti-inflammatory effect was noted for pro-inflammatory cytokine (TNF α , IL-1 β and IL-6) secretion as well. Within this timeframe of 24 h, PLGA-coated BAG-S53P4 scaffolds showed a decreased anti-inflammatory effect compared with non-coated BAG-S53P4 scaffolds rather than producing a pro-inflammatory reaction. This is in contrast to a previous study, where, in a short-term (4 h) experiment, PLGA microparticles produce an pro-inflammatory reaction *in vitro* on murine macrophages (Nicolette *et al.*, 2011). However, the immunomodulatory effects of PLGA have also been

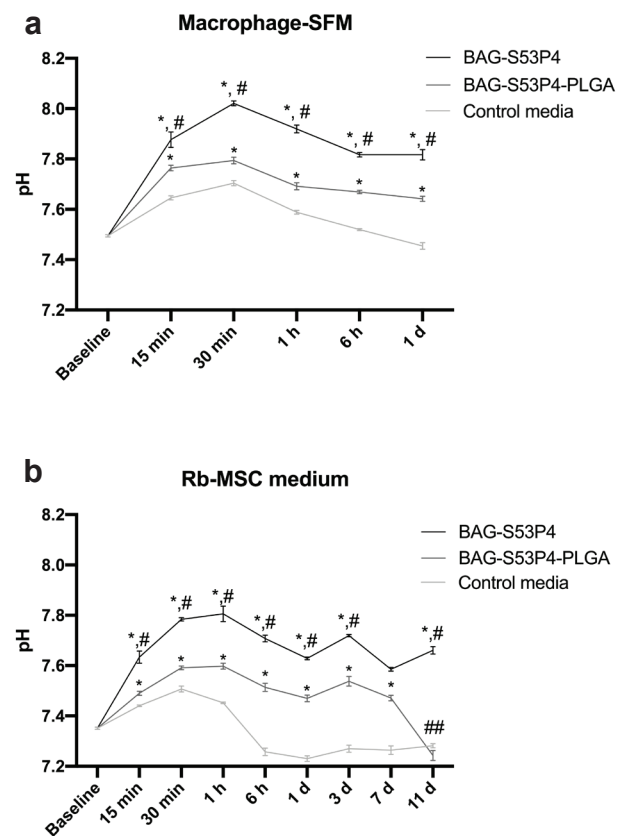


Fig. 9. Time-course pH measurements of macrophage-SFM and Oricell basal MSC growth media (BM) incubated with BAG-S53P4 (\pm PLGA) scaffolds. The experiment was conducted in the absence of cells. (a) pH measurements in macrophage-SFM and (b) pH measurements in BM. * = statistical significance ($p < 0.05$) compared with control, # = statistical significance ($p < 0.05$) of BAG-S53P4 vs. BAG-S53P4-PLGA, and ## = statistical significance ($p < 0.05$) of BM vs. BAG-S53P4-PLGA.

shown to be immunosuppressive in dendritic cells exposed to PLGA microparticles for longer periods (up to 120 h) (Allen *et al.*, 2018). Considering these contrasting reports, the overall immunomodulatory effect of PLGA warrants further research.

In previous *in vivo* experiments, differences were demonstrated in the IM characteristics with regards to TNF α , VEGF and BMP expression between coated and non-coated BAG-S53P4 scaffolds without any obvious deleterious effects (Björkenheim *et al.*, 2017; Björkenheim *et al.*, 2019). The rationale behind the rapid degradation profile of the utilised PLGA – minimum of 14 d (Cyphert *et al.*, 2020) – was to allow the BAG-S53P4 to interact with the surroundings as early as possible to hinder the formation of a fibrotic capsule. These findings were hypothesised to be due to a stronger initial inflammatory reaction of PLGA-coated scaffolds compared to uncoated BAG-S53P4 scaffolds alone, leading to a formation of a biologically more active IM. The current results suggested that the PLGA coating functioned mainly by inhibiting and slowing down the native BAG surface reactions, which thus attenuated the innate anti-inflammatory

properties of BAGs rather than directly inducing an inflammatory reaction. These apparently conflicting results might partially be explained by PLGA-degradation dynamics. In the relatively short time frame of the current study, only small amounts of the PLGA degradation products were likely released into the cell culture media, while in the *in vivo* experiments the whole coating was eventually degraded. The potential immunomodulatory properties of higher concentrations of PLGA degradation products, as well as the consequences of extended exposure to them, remain a topic for further research. Although further studies are warranted, it can be proposed that the net *in vivo* effect of the PLGA coating is initially pro-inflammatory, possibly due to both inhibition of BAG anti-inflammatory properties and the short-term pro-inflammatory action; at later stages, the effect is anti-inflammatory. Taken together, the sintered BAG scaffolds seem to have anti-inflammatory properties that are partially inhibited or at least slowed down by the PLGA coating. However, as previously demonstrated (Björkenheim *et al.*, 2017; Björkenheim *et al.*, 2019), sintered BAG-S53P4 scaffolds can induce a biologically active membrane in rabbits by having a limited inflammatory effect *in vivo*. Thus, the actions of BAG-S53P4 are deemed as immunomodulatory rather than purely anti-inflammatory. The immunomodulatory results are consistent with previous BAG studies, although these reports have been conducted using different types of BAGs and cells (Kim *et al.*, 2019; Varmette *et al.*, 2009).

Although granules of BAG-S53P4 are known to have good biocompatibility and are currently used in clinical practice (Lindfors *et al.*, 2010b), some cytotoxicity was still observed in the scaffold-containing macrophage cultures. This slightly increased cell death rate (non-significant) of scaffold-stimulated macrophages likely occurred due to unavoidable mechanical friction caused by the scaffold, as the scaffolds were placed directly on top of the cells partially covering the well surface. In fact, some areas of detached cells were observed underneath the scaffolds when the scaffold was removed from the wells. This probably could have been avoided by using a trans-well culture system. However, the apical pressure effect of the scaffolds on the cells would also seem to be minimal in the experimental setting, and the utilisation of a trans-well setting would probably have yielded a similar result. It has been proposed that cell stimulation with BAGs leads to cellular death, due to alkalinisation of the surrounding environment. Pre-conditioning of BAG by incubation in the cell culture media prior to *in vitro* experiments has also been suggested (Ciraldo *et al.*, 2018). However, no differences were found in cytotoxicity induced by pre-conditioned and non-preconditioned BAG-S53P4 (\pm PLGA) scaffolds in preliminary experiments (data not shown). Scaffold pre-conditioning was further confirmed to be non-significant in terms of its immunomodulatory effect (data not shown). Therefore, non-preconditioned

BAG scaffolds were selected for the cell culture models. Of note, this approach has also been used in previous *in vivo* studies (Björkenheim *et al.*, 2017; Björkenheim *et al.*, 2019). Moreover, the results obtained might have been affected by the tendency of LPS to bind to the scaffold surfaces. Regardless, it is believed that the effect of these factors remained relatively modest and could not alone account for the striking immunomodulatory effects detected for BAG scaffolds.

It has previously been reported that BAG-S53P4 can induce an active membrane with osteogenic potential (Björkenheim *et al.*, 2019). Furthermore, BAG-S53P4 in granular form is associated with direct osteostimulative properties (Waselau *et al.*, 2012). In the present study, sintered BAG-S53P4 scaffolds induced osteogenic differentiation of Rb-MSCs; at an early 3 d timepoint elevated mRNA expression levels of *RUNX2*, *FMOD*, and *OGN* were already observed. Of these markers, transcription factor *RUNX2* promotes differentiation of MSCs into osteoblasts, whereas *FMOD* represents a biomarker associated with the maturation process of osteoprogenitor cells (Banerjee *et al.*, 1997; Waddington *et al.*, 2003). *OGN* reportedly plays a role in later stages of the osteoblast maturation process (Tanaka *et al.*, 2012). Strikingly, the expression levels of BAG-S53P4-induced osteogenic markers were comparable to those induced by osteogenic media. In the mineralisation assay, an attempt was made to identify if the mineralisation manifested earlier in Rb-MSCs stimulated with BAG-S53P4 (\pm PLGA) scaffolds, when compared with cells cultured in OM alone. According to the pilot study and supplier's recommendation, a 14 d period is sufficient for Rb-MSC mineralisation. Ojansivu *et al.* also used a 11 d to 14 d stimulation time when evaluating mineralisation from BAG extracts (Ojansivu *et al.*, 2015). Furthermore, Rb-MSC have been shown to have a higher osteogenic potential than hMSCs (Tan *et al.*, 2013). Thus, this 11 d time point was selected to evaluate if BAG-S53P4 (\pm PLGA) scaffolds produced mineralisation even earlier than control samples and to evaluate the possible difference between the non-coated and PLGA coated BAG-S53P4 scaffolds in Rb-MSCs. At the 11 d timepoint, mineralisation was clearly present for BAG-S53P4-stimulated Rb-MSCs, whereas mineralisation of Rb-MSCs treated with OM or BAG-S53P4-PLGA scaffolds remained low. Of note, this mineralisation was observed at the site of scaffold and at sites where scaffold was not present. Mineralisation measurement (AR stain) with BAG-S53P4 (\pm PLGA) scaffolds without cells revealed some mineralisation as well, but this mineralisation only occurred at the site where the scaffold had been present. The results were consistent with a previous report suggesting that non-sintered BAG-S53P4 is capable of inducing osteogenic differentiation (Ojansivu *et al.*, 2018; Ojansivu *et al.*, 2015).

The exact cell biological mechanisms underlying the observed immunomodulatory and osteogenic

properties of BAG-S53P4 scaffolds remain to be elucidated but are likely attributable to the dissolution of the BAG and the corresponding alkalisation of the local environment and release of Ca, Si and P species. For example, an alkaline environment affects macrophages by inhibiting the IL-1 β response to several known inflammatory activators (Rajamäki *et al.*, 2013) and increases osteoblast viability (Galow *et al.*, 2017). Furthermore, extracellular Ca ions and Si species have been shown to have anti-inflammatory effects on murine macrophages (Huang *et al.*, 2018) and to promote osteogenic differentiation of MSCs (Barradas *et al.*, 2012; Lin *et al.*, 2013). Additionally, elevated Ca-ion concentrations have been shown to enhance angiogenesis (Wu *et al.*, 2009) with the Ca to Si ratio also playing a role in the angiogenic capacity (Li and Chang, 2013), thus warranting future research in the direct angiogenic capability of BAG-S53P4 (\pm PLGA) scaffolds.

The alkalisation of the local cell medium was observed in both macrophage and Rb-MSC media when incubated with BAG-S53P4 (\pm PLGA) scaffolds. BAG-S53P4 showed significantly elevated pH compared with BAG-S53P4-PLGA and control cell media. In addition, both scaffolds demonstrated release of ion concentrations that were consistent with previous reports (Fagerlund *et al.*, 2013). The difference in osteogenic induction between BAG-S53P4 and BAG-S53P4-PLGA scaffolds may be partially explained by differences in their ionic dissolution patterns. Indeed, in this experimental setting, BAG-S53P4 scaffolds without a PLGA coating showed elevated Si and Ca concentrations in the ionic dissolution analysis, with PLGA coating probably acting as a mechanical barrier to hinder the actions of the BAG. Moreover, the lower values of P species in the ionic dissolution for BAG-S53P4 compared with BAG-S53P4-PLGA would support greater mineralisation/surface precipitation in the former group. This proposal is supported by SEM imaging, which revealed clear Ca-P reaction layers on the outer parts of the uncoated BAG particles of BAG-S53P4 scaffolds. This reactivity remained minimal at the surfaces of the polymer-coated BAG-S53P4-PLGA within the time frame studied.

These results demonstrated a proof of principle that the biological activity of BAG scaffolds could be modulated with the application of PLGA coating. The coating functioned not by directly inducing inflammation but by slowing down the BAG surface reactions and inhibiting the strong anti-inflammatory properties of the material. The delayed reactivity of the BAG-S53P4-PLGA scaffold may be beneficial for the formation of an IM and subsequent bone regeneration. This mechanism of action allows a period of initial inflammation followed by extended anti-inflammatory and osteogenic effects as the PLGA coating gradually degrades, revealing the surface of the BAG. Indeed, prior *in vivo* observations partially support this hypothesis (Björkenheim *et al.*, 2017; Björkenheim *et al.*, 2019). Of note, care must be taken

when implementing novel bioactive materials into clinical practise. Regarding PLGA implants (*e.g.* interference screws), long term adverse effects have been documented – such as material fragmentation, incomplete degradation, adverse foreign body response, and cyst formation (Chevallier *et al.*, 2019; Cox *et al.*, 2014). However, these applications are different from the currently studied one and do not necessarily reflect the properties of the relatively thin PLGA coating.

Conclusions

Sintered BAG-S53P4 scaffolds demonstrated an immunomodulatory property on human macrophages that, as far as is known, has not been previously described. Furthermore, it was shown that sintered BAG-S53P4 scaffolds had direct osteogenic stimulatory effects on rabbit MSCs *in vitro*. These results were likely attributable to the alkalisation of the surroundings and the release of the biologically active Si, Ca and P species from the scaffold. These dynamics could be significantly modulated by application of a PLGA coating on the scaffold surface. Contrary to the initial hypothesis, the PLGA coating did not induce a stronger inflammatory response when compared to uncoated BAG. The result indicated that it served as a biodegradable barrier that attenuated BAG ion release and innate immunomodulatory and osteogenic effects. These results supported the role of coating BAG-S53P4 scaffolds with a biodegradable polymer, such as PLGA, to tune the immunomodulatory and osteogenic responses and consequently allow tailoring of the scaffold properties to meet the specific clinical need.

References

- Allen RP, Bolandparvaz A, Ma JA, Manickam VA, Lewis JS (2018) Latent, immunosuppressive nature of poly(lactic-co-glycolic acid) microparticles. *ACS Biomater Sci Eng* **4**: 900-918.
- Arend WP, Malyak M, Guthridge CJ, Gabay C (1998) Interleukin-1 receptor antagonist: role in biology. *Annu Rev Immunol* **16**: 27-55.
- Baino F, Hamzehlou S, Kargozar S (2018) Bioactive glasses: where are we and where are we going? *J Funct Biomater* **9**: 25. DOI: 10.3390/jfb9010025.
- Banerjee C, McCabe LR, Choi JY, Hiebert SW, Stein JL, Stein GS, Lian JB (1997) Runt homology domain proteins in osteoblast differentiation: AML3/CBFA1 is a major component of a bone-specific complex. *J Cell Biochem* **66**: 1-8.
- Barnes GL, Kostenuik PJ, Gerstenfeld LC, Einhorn TA (1999) Growth factor regulation of fracture repair. *J Bone Miner Res* **14**: 1805-1815.
- Barradas AMC, Fernandes HAM, Groen N, Chai YC, Schrooten J, van de Peppel J, van Leeuwen JPTM,

- van Blitterswijk CA, de Boer J (2012) A calcium-induced signaling cascade leading to osteogenic differentiation of human bone marrow-derived mesenchymal stromal cells. *Biomaterials* **33**: 3205-3215.
- Björkenheim R, Strömberg G, Pajarinen J, Ainola M, Uppstu P, Hupa L, Böhling TO, Lindfors NC (2017) Polymer-coated bioactive glass S53P4 increases VEGF and TNF expression in an induced membrane model *in vivo*. *J Mater Sci* **52**: 9055-9065.
- Björkenheim R, Strömberg G, Ainola M, Uppstu P, Aalto-Setälä L, Hupa L, Pajarinen J, Lindfors NC (2019) Bone morphogenic protein expression and bone formation are induced by bioactive glass S53P4 scaffolds *in vivo*. *J Biomed Mater Res B Appl Biomater* **107**: 847-857.
- Chen QZ, Boccaccini AR (2006) Poly(D,L-lactic acid) coated 45S5 Bioglass-based scaffolds: processing and characterization. *J Biomed Mater Res A* **77**: 445-457.
- Chevallier R, Klouche S, Gerometta A, Bohu Y, Herman S, Lefevre N (2019) Bioabsorbable screws, whatever the composition, can result in symptomatic intra-osseous tibial tunnel cysts after ACL reconstruction. *Knee Surg Sports Traumatol Arthrosc* **27**: 76-85.
- Ciraldo FE, Boccardi E, Melli V, Westhauser F, Boccaccini AR (2018) Tackling bioactive glass excessive *in vitro* bioreactivity: Preconditioning approaches for cell culture tests. *Acta Biomater* **75**: 3-10.
- Cox CL, Spindler KP, Leonard JP, Morris BJ, Dunn WR, Reinke EK (2014) Do newer-generation bioabsorbable screws become incorporated into bone at two years after ACL reconstruction with patellar tendon graft?: a cohort study. *J Bone Joint Surg Am* **96**: 244-250.
- Cyphert EL, Bil M, Recum von HA, Świążkowski W (2020) Repurposing biodegradable tissue engineering scaffolds for localized chemotherapeutic delivery. *J Biomed Mater Res A* **108**: 1144-1158.
- Day RM, Boccaccini AR (2005) Effect of particulate bioactive glasses on human macrophages and monocytes *in vitro*. *J Biomed Mater Res A* **73**: 73-79.
- Einhorn TA, Majeska RJ, Rush EB, Levine PM, Horowitz MC (1995) The expression of cytokine activity by fracture callus. *J Bone Miner Res* **10**: 1272-1281.
- Fagerlund S, Hupa L, Hupa M (2013) Dissolution patterns of biocompatible glasses in 2-amino-2-hydroxymethyl-propane-1,3-diol (Tris) buffer. *Acta Biomater* **9**: 5400-5410.
- Fagerlund S, Massera J, Moritz N, Hupa L, Hupa M (2012) Phase composition and *in vitro* bioactivity of porous implants made of bioactive glass S53P4. *Acta Biomater* **8**: 2331-2339.
- Galow A-M, Rebl A, Koczan D, Bonk SM, Baumann W, Gimsa J (2017) Increased osteoblast viability at alkaline pH *in vitro* provides a new perspective on bone regeneration. *Biochem Biophys Rep* **10**: 17-25.
- Gerstenfeld LC, Cho TJ, Kon T, Aizawa T, Tsay A, Fitch J, Barnes GL, Graves DT, Einhorn TA (2003) Impaired fracture healing in the absence of TNF-alpha signaling: the role of TNF-alpha in endochondral cartilage resorption. *J Bone Miner Res* **18**: 1584-1592.
- Giannoudis PV, Einhorn TA, Marsh D (2007) Fracture healing: the diamond concept. *Injury* **38 Suppl 4**: S3-S6.
- Gruber HE, Ode G, Hoelscher G, Ingram J, Bethea S, Bosse MJ (2016) Osteogenic, stem cell and molecular characterisation of the human induced membrane from extremity bone defects. *Bone Joint Res* **5**: 106-115.
- Hench LL, Paschall HA (1973) Direct chemical bond of bioactive glass-ceramic materials to bone and muscle. *J Biomed Mater Res* **7**: 25-42.
- Hench LL, Polak JM, Xynos ID, Bותרy LDK (2000) Bioactive materials to control cell cycle. *Mater Res Innov* **3**: 313-323.
- Hench LL, Xynos ID, Polak JM (2004) Bioactive glasses for *in situ* tissue regeneration. *J Biomater Sci Polym Ed* **15**: 543-562.
- Hoppe A, Güldal NS, Boccaccini AR (2011) A review of the biological response to ionic dissolution products from bioactive glasses and glass-ceramics. *Biomaterials* **32**: 2757-2774.
- Huang Y, Wu C, Zhang X, Chang J, Dai K (2018) Regulation of immune response by bioactive ions released from silicate bioceramics for bone regeneration. *Acta Biomater* **66**: 81-92.
- Jones JR (2013) Review of bioactive glass: from Hench to hybrids. *Acta Biomater* **9**: 4457-4486.
- Kankare J, Lindfors NC (2016) Reconstruction of vertebral bone defects using an expandable replacement device and bioactive glass S53P4 in the treatment of vertebral osteomyelitis: three patients and three pathogens. *Scand J Surg* **105**: 248-253.
- Kim T-H, Kang MS, Mandakhbayar N, El-Fiqi A, Kim H-W (2019) Anti-inflammatory actions of folate-functionalized bioactive ion-releasing nanoparticles imply drug-free nanotherapy of inflamed tissues. *Biomaterials* **207**: 23-38.
- Lange J, Sapozhnikova A, Lu C, Hu D, Li X, Miclau T, Marcucio RS (2010) Action of IL-1beta during fracture healing. *J Orthop Res* **28**: 778-784.
- Leppäranta O, Vahtio M, Peltola T, Zhang D, Hupa L, Hupa M, Ylänen H, Salonen JI, Viljanen MK, Eerola E (2008) Antibacterial effect of bioactive glasses on clinically important anaerobic bacteria *in vitro*. *J Mater Sci Mater Med* **19**: 547-551.
- Li H, Chang J (2013) Stimulation of proangiogenesis by calcium silicate bioactive ceramic. *Acta Biomater* **9**: 5379-5389.
- Lin K, Xia L, Li H, Jiang X, Pan H, Xu Y, Lu WW, Zhang Z, Chang J (2013) Enhanced osteoporotic bone regeneration by strontium-substituted calcium silicate bioactive ceramics. *Biomaterials* **34**: 10028-10042.
- Lindfors NC, Hyvönen P, Nyssönen M, Kirjavainen M, Kankare J, Gullichsen E, Salo J (2010a)

Bioactive glass S53P4 as bone graft substitute in treatment of osteomyelitis. *Bone* **47**: 212-218.

Lindfors NC, Heikkilä JT, Koski I, Mattila K, Aho AJ (2009) Bioactive glass and autogenous bone as bone graft substitutes in benign bone tumors. *J Biomed Mater Res B Appl Biomater* **90**: 131-136.

Lindfors NC, Koski I, Heikkilä JT, Mattila K, Aho AJ (2010b) A prospective randomized 14-year follow-up study of bioactive glass and autogenous bone as bone graft substitutes in benign bone tumors. *J Biomed Mater Res B Appl Biomater* **94**: 157-164.

Loi F, Córdova LA, Pajarinen J, Lin T-H, Yao Z, Goodman SB (2016) Inflammation, fracture and bone repair. *Bone* **86**: 119-130.

Magri AMP, Fernandes KR, Assis L, Kido HW, Avanzi IR, Medeiros MDC, Granito RN, Braga FJC, Rennó ACM (2019) Incorporation of collagen and PLGA in bioactive glass: *in vivo* biological evaluation. *Int J Biol Macromol* **134**: 869-881.

Mantsos T, Chatzistavrou X, Roether JA, Hupa L, Arstila H, Boccaccini AR (2009) Non-crystalline composite tissue engineering scaffolds using boron-containing bioactive glass and poly(D,L-lactic acid) coatings. *Biomed Mater* **4**: 055002. DOI: 10.1088/1748-6041/4/5/055002.

Masquelet AC, Fitoussi F, Begue T, Muller GP (2000) [Reconstruction of the long bones by the induced membrane and spongy autograft]. *Ann Chir Plast Esthet* **45**: 346-353.

Munukka E, Leppäranta O, Korkeamäki M, Vahtio M, Peltola T, Zhang D, Hupa L, Ylänen H, Salonen JI, Viljanen MK, Eerola E (2008) Bactericidal effects of bioactive glasses on clinically important aerobic bacteria. *J Mater Sci Mater Med* **19**: 27-32.

Nicolette R, Santos dos DF, Faccioli LH (2011) The uptake of PLGA micro or nanoparticles by macrophages provokes distinct *in vitro* inflammatory response. *Int Immunopharmacol.* **11**: 1557-1563.

Nurmi K, Kareinen I, Virkanen J, Rajamäki K, Kouri V-P, Vaali K, Levonen A-L, Fyhrquist N, Matikainen S, Kovanen PT, Eklund KK (2017) Hemin and cobalt protoporphyrin inhibit NLRP3 inflammasome activation by enhancing autophagy: a novel mechanism of inflammasome regulation. *J Innate Immun* **9**: 65-82.

Ojansivu M, Hyväri L, Kellomäki M, Hupa L, Vanhatupa S, Miettinen S (2018) Bioactive glass induced osteogenic differentiation of human adipose stem cells is dependent on cell attachment mechanism and mitogen-activated protein kinases. *Eur Cell Mater* **35**: 54-72.

Ojansivu M, Vanhatupa S, Björkvik L, Häkkänen H, Kellomäki M, Autio R, Ihalainen JA, Hupa L, Miettinen S (2015) Bioactive glass ions as strong enhancers of osteogenic differentiation in human adipose stem cells. *Acta Biomater* **21**: 190-203.

Pelissier P, Masquelet AC, Bareille R, Pelissier SM, Amedee J (2004) Induced membranes secrete growth factors including vascular and osteoinductive factors and could stimulate bone regeneration. *J Orthop Res* **22**: 73-79.

Rajamäki K, Nordström T, Nurmi K, Åkerman KEO, Kovanen PT, Öörni K, Eklund KK (2013) Extracellular acidosis is a novel danger signal alerting innate immunity *via* the NLRP3 inflammasome. *J Biol Chem* **288**: 13410-13419.

Shi Q, Li ZY, Liverani L, Roether J, Chen Q, Boccaccini AR (2018) Positive effect of wrapping poly caprolactone/polyethylene glycol fibrous films on the mechanical properties of 45S5 bioactive glass scaffolds. *Int J Appl Ceram Technol* **15**: 921-929.

Stoor P, Söderling E, Salonen JI (1998) Antibacterial effects of a bioactive glass paste on oral microorganisms. *Acta Odontol Scand* **56**: 161-165.

Stoor P, Pulkkinen J, Grénman R (2010) Bioactive glass S53P4 in the filling of cavities in the mastoid cell area in surgery for chronic otitis media. *Ann Otol Rhinol Laryngol* **119**: 377-382.

Tan S-L, Ahmad TS, Selvaratnam L, Kamarul T (2013) Isolation, characterization and the multilineage differentiation potential of rabbit bone marrow-derived mesenchymal stem cells. *J Anat* **222**: 437-450.

Tanaka K-I, Matsumoto E, Higashimaki Y, Katagiri T, Sugimoto T, Seino S, Kaji H (2012) Role of osteoglycin in the linkage between muscle and bone. *J Biol Chem* **287**: 11616-11628.

Tanner MC, Heller R, Westhauser F, Miska M, Ferbert T, Fischer C, Gantz S, Schmidmaier G, Haubruck P (2018) Evaluation of the clinical effectiveness of bioactive glass (S53P4) in the treatment of non-unions of the tibia and femur: study protocol of a randomized controlled non-inferiority trial. *Trials* **19**: 299. DOI: 10.1186/s13063-018-2681-9.

Varmette EA, Nowalk JR, Flick LM, Hall MM (2009) Abrogation of the inflammatory response in LPS-stimulated RAW 264.7 murine macrophages by Zn- and Cu-doped bioactive sol-gel glasses. *J Biomed Mater Res A* **90**: 317-325.

Waddington RJ, Roberts HC, Sugars RV, Schönherr E (2003) Differential roles for small leucine-rich proteoglycans in bone formation. *Eur Cell Mater* **6**: 12-21.

Waselau M, Patrikoski M, Juntunen M, Kujala K, Kääriäinen M, Kuokkanen H, Sándor GK, Vapaavuori O, Suuronen R, Mannerström B, Rechenberg von B, Miettinen S (2012) Effects of bioactive glass S53P4 or beta-tricalcium phosphate and bone morphogenetic protein-2 and bone morphogenetic protein-7 on osteogenic differentiation of human adipose stem cells. *J Tissue Eng* **3**: 2041731412467789. DOI: 10.1177/2041731412467789.

Wilson J, Low SB (1992) Bioactive ceramics for periodontal treatment: comparative studies in the Patus monkey. *J Appl Biomater* **3**: 123-129.

Wu Q, Shao H, Li J, Li J, Yang B, Webster KA, Yu H (2009) Extracellular calcium increases CXCR4 expression on bone marrow-derived cells and enhances pro-angiogenesis therapy. *J Cell Mol Med* **13**: 3764-3773.

Xynos ID, Hukkanen MV, Batten JJ, Buttery LD, Hench LL, Polak JM (2000) Bioglass 45S5 stimulates

osteoblast turnover and enhances bone formation *in vitro*: implications and applications for bone tissue engineering. *Calcif Tissue Int* **67**: 321-329.

Xynos ID, Edgar AJ, Buttery LDK, Hench LL, Polak JM (2001) Gene-expression profiling of human osteoblasts following treatment with the ionic products of Bioglass® 45S5 dissolution. *J Biomed Mater Res* **55**: 151-157.

Zhang D, Leppäranta O, Munukka E, Ylänen H, Viljanen MK, Eerola E, Hupa M, Hupa L (2010) Antibacterial effects and dissolution behavior of six bioactive glasses. *J Biomed Mater Res A* **93**: 475-483.

Zomer HD, Roballo KC, Lessa TB, Bressan FF, Gonçalves NN, Meirelles FV, Trentin AG, Ambrósio CE (2018) Distinct features of rabbit and human adipose-derived mesenchymal stem cells: implications for biotechnology and translational research. *Stem Cells Cloning* **11**: 43-54.

Discussion with Reviewer

Noel Davison: What was the rationale of using rabbit MSCs in this study?

Authors: The rabbit MSCs were chosen for practical reasons; they are commercially available, relatively low cost and simple to culture. Most importantly, however, they have been shown to be a reasonable model system for hMSCs (Zomer *et al.*, 2018.) and have been used in studies in the field of biomaterial research (Guo *et al.*, 2009, additional reference).

Noel Davison: There are a number of scaffold properties that may influence the inflammatory response; how might the authors identify the role of single or multiple parameters/properties (*e.g.* pH, ion release, surface apatite formation) of the scaffolds described here might play in this?

Authors: The immunomodulatory effect of the BAG scaffolds are indeed multifaceted. Since the immunomodulatory effects were demonstrated in the current study in an indirect culture model, those must be attributable to release of soluble substances from the scaffold, rather than direct interaction of scaffold surface with the cells. Since the composition of the BAG is well characterised, the soluble immunomodulatory factors released from the scaffold must be various ions, elevation in the local pH or, possibly, some combination of these. For example, elevation of local pH has been shown to inhibit inflammasome activation and could also potentially inhibit other pro-inflammatory signalling pathways such as NF- κ B (Rajamäki *et al.*, 2013). Additionally, ions released from the scaffold (Ca, Si) have been shown to downregulate inflammation in macrophage cell cultures (Huang *et al.*, 2018). A step-by-step analysis on how each of these factors alone, and in combination with other factors, could be conducted in simple macrophage cell culture model is needed. In addition, it would be useful to study the direct immunomodulatory effects of the scaffolds, macrophages and other cells that could be grown directly on the scaffold surfaces, before and after the layer of HA has been formed. These experiments are currently ongoing.

Additional Reference

Guo X, Park H, Liu G, Liu W, Cao Y, Tabata Y, Kasper FK, Mikos AG (2009) *In vitro* generation of an osteochondral construct using injectable hydrogel composites encapsulating rabbit marrow mesenchymal stem cells. *Biomaterials* **30**: 2741-2752.

Editor's note: The Scientific Editor responsible for this paper was Joost de Bruijn.